Application Note 40

Photoresponse Mapping of Photovoltaic Cells

Technology and Applications Center
Newport Corporation

Spectra-Physics
A Division of Newport Corporation

Newport
Experience | Solutions

Introduction

The performance of a photovoltaic (PV) cell can be quantified by measuring its spectral response and I-V curve. From these measurements the parameters like external quantum efficiency (EQE%), fill factor, efficiency, and maximum power can be derived[1]. For example, efficiency η of the cell is calculated as

$$\eta = 100 \times \frac{P_m}{A E_o}, \quad (1)$$

where P_m is the maximum power (W), A is the cell area (m^2) and E_o is the standard reporting irradiance (W/m^2).

It is evident that accurately calculating the efficiency depends on how accurately the area A of the PV cell is known. In most of the cases the area is measured using visual methods with the assumption that the cell has a uniform response over the entire area. However, despite the fact that the cell may look uniform visually, significant non-uniformity of the photoresponse over the cell area is possible. This tends to be the case in the research environment when the manufacturing processes are not worked out, or when degradation of the cell occurs. For EQE% measurements in general the actual illuminated area of the cell is usually much smaller than the defined area of the cell. Thus, depending on the position of the illuminated area used for EQE% measurements significant differences in results can be expected. An example of an organic PV cell is shown in Figure 1a.

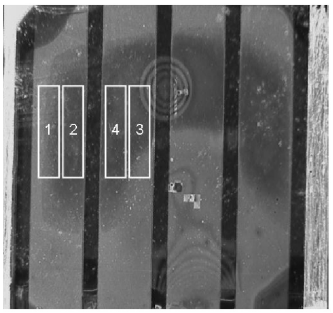

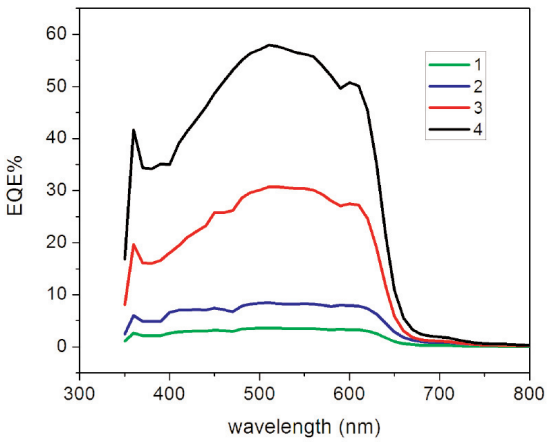

Figure 1. (a) Photo of the organic PV cell with area of the cell used for recording EQE% . (b) EQE% scans corresponding to areas 1-4.

Measurement of EQE% in four different spots (1-4) exhibits an order of magnitude difference as shown in Figure 1b. If one assumes that the entire surface of the cell is uniform and then measures the I-V curve by illuminating the entire surface of the cell with 1 Sun of irradiance (1000 W/m^2), an artificially low value of the efficiency will be calculated. Thus, the photoresponse uniformity data can be used to improve manufacturing processes by exposing discontinuities in a cell's photoresponse due to cracks and/or contamination, or degradation in the case of organic PV cells[6].

The photoresponse mapping technique is a simpler version of what has come to be known in the literature as Laser Beam Induced Current or LBIC[2,3]. In LBIC the laser beam is focused onto the PV cell surface using a microscope objective lens. To avoid challenges due to surface roughness and non-flatness of the sample surface a careful polishing[4] or auto-focus[5] were proposed.

In this application note we describe a simple and cost effective device based on standard Newport components that facilitates photocurrent mapping of PV cells or modules with dimensions up to 8"x 8".

Experimental setup

The diagram of the setup and the picture of the actual device are shown in Figure 2 and Figure 3.

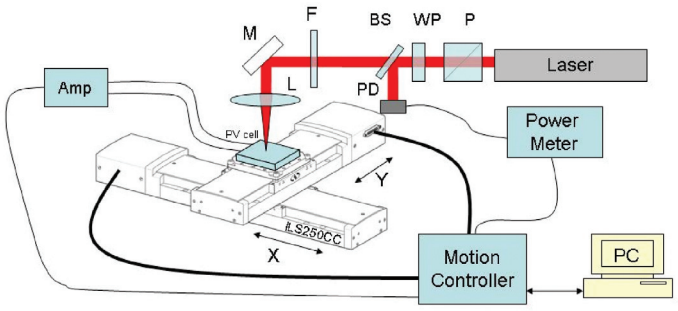

Figure 2 Schematic diagram of the set-up. P - polarizer, WP - _ wave plate, PD - photodiode, F - filter wheel, M - turning mirror, L - focusing lens, BS - beamsplitter.

For illumination of the samples we used three different lasers with wavelengths 633nm (2mW HeNe, R-33142), 532 nm (EXLSR-532-50-CDRH), and 375 nm (EXLSR-375C-16). The laser beam is directed to the sample after passing through an isolator made up of polarizer P and a 1/4 wave plate WP. The focusing lens L is a fused silica plano-convex lens with a focal length of 50 mm. We measured the spot size at the sample to be in the range of 0.1-0.2 mm at the beam waist ($1/e^2$).

In general, a shorter focal length lens or microscope objective can be used to achieve higher spatial resolution at the expense of longer scanning time. For the purpose of having a reasonable scan time of 0.2 min/mm^2 and be able to map the entire cell in all experiments we limited our resolution to 0.1-0.2 mm. The beam was attenuated using ND

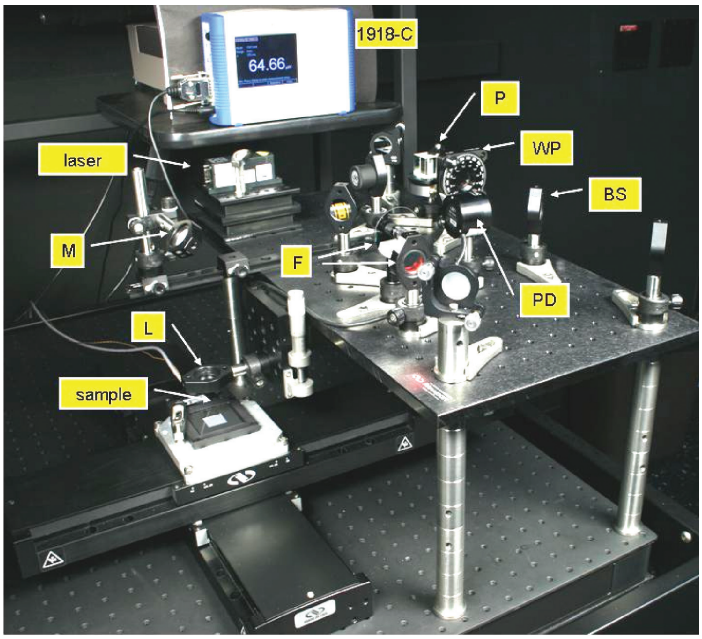

Figure 3. A picture of the PV cell scanner. XPS motion controller not shown. BS - beamsplitter. P - polarizer, WP - _ wave plate, PD - photodiode, F - filter wheel, M - turning mirror, L - focusing lens, BS - beamsplitter

filter wheel F (Newport 50FS04DV.4) to deliver 100 mW/cm^2 (1 Sun of irradiance) onto the cell. For a reference channel a small portion of the beam is picked-off after the isolator and the average power is recorded using a Newport 1918-C power meter and a 918D-UV-OD3 photodiode. The PV cell was mounted on top of two computer controlled linear stages (ILS250CC) providing XY positioning of the cell in the XY plane normal to the laser beam with an accuracy of 2.5 microns. We used a 2-axis XPS Series Controller/Driver to control the stages. The generated photocurrent for each XY position is pre-amplified and converted into voltage using an Oriel® Current Preamplifier (70710). The data is sampled at 10 kHz by one of four analog DAQ inputs through a GPIO port on the back of the XPS. Example LabVIEW® based software provided with the device allows monitoring of the scan in real time. Both 3D and contour plots are available. Assembly details are given in a subsequent section in this Application Note.

Experimental results

We investigated photoresponse maps of three types of cells: a commercially available mono-crystalline silicon cell, an experimental CIGS and an organic P3HT/C60 cell. First EQE% was recorded using Newport's QE/IPCE Measurement Kit (Newport QE-PV-SI). The results are presented in Figure 4. It is evident that the photoresponse of each cell exhibits a different dependence on wavelength of the laser. On the other hand, the penetration depth of the laser beam into the cell also depends on wavelength. The colored lines in Figure 4 correspond to wavelengths of the lasers used in the experiments, so that the photoresponse scan can be thought of as an EQE% scan at one wavelength over the entire surface of the cell.

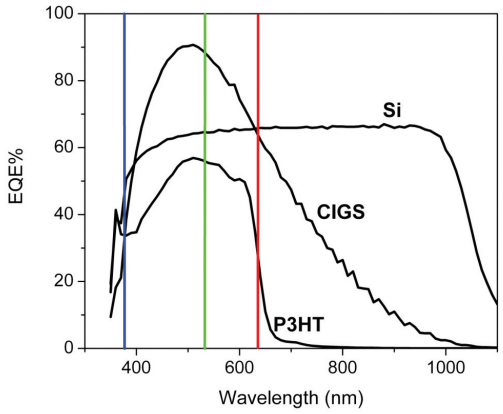

Figure 4. Measured EQE% of the various PV cells by the Newport QE/IPCE Measurement Kit. Vertical color lines correspond to wavelengths of the lasers used in the experiment.

For example, the 375 nm laser beam will be absorbed in the first 10-20 nm of the material, while the 632 nm beam will penetrate much deeper. Thus, despite the fact that Rayleigh length of the laser beam at the focus is about 0.5 mm long, varying the wavelength of the laser allows selective probing of the cell at different depths. Figure 5 shows a picture and a photoresponse map of the Si cell taken at the three wavelengths. The colors represent photocurrent and are in arbitrary units.

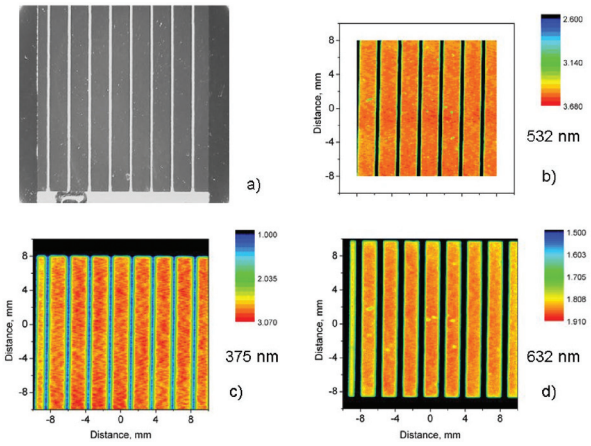

Figure 5. Photograph of the Si cell and photocurrent maps at 532 nm, 375 nm and 632nm.

The uniformity maps are very similar and the photoresponse is fairly uniform across the entire surface area of the cell, but there are clearly observable spots with reduced or no photoresponse due to inclusions, dust or damage to the cell

or to the protective window. Common features are visible at all wavelengths; the 375nm scan being noisier due to reduced photocurrent and higher gain setting on the preamplifier. The image of the contacts is sharper on the 532 nm plot due to smaller spot size (due to better collimation and focus).

The photocurrent map of a section of the CIGS cell scanned with 632 nm is shown in Figure 6. A slight fall off of the photoresponse on the right side is observable, and there are multiple spots with reduced photoresponse.

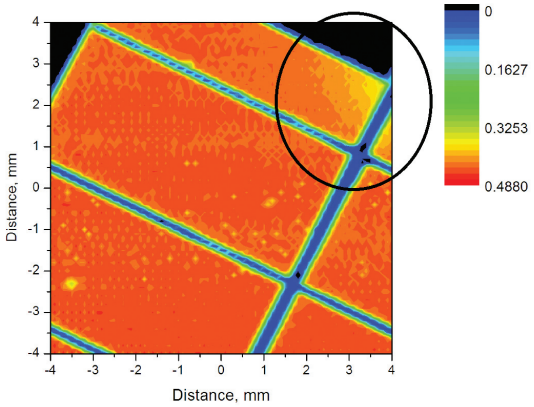

Figure 6. A photoresponse scan of the experimental CIGS PV cell. A drop off of the signal is seen in the upper right-hand corner even though upon visual inspection the cell appeared to be uniform. The colors represent photocurrent and are in arbitrary units.

In this case, the non-uniformity of the response will have little effect on efficiency calculations, but the data can be used to reveal imperfections in the structure or in the packaging.

Finally, the photoresponse data and picture of the experimental organic cell are shown in Figure 7.

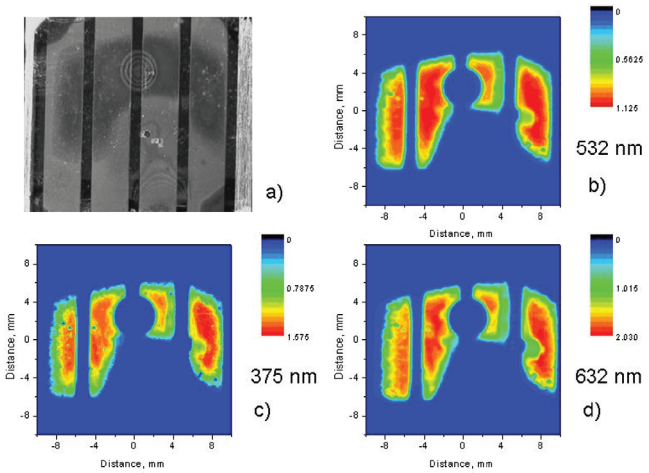

Figure 7. Photograph (a) and photocurrent maps of an organic PV cell at different wavelengths: 532 nm (b), 375 nm (c) and 632 nm (d).

Organic cells are known to be sensitive to UV light and exposure to oxygen, and have a tendency to slowly degrade if packaging is not done carefully. The changes are visible on the picture of the cell in Figure 7a. Non-uniformity of the photoresponse is confirmed in wavelength dependent photoresponse maps in Figure 7(b-d). Figure 8 shows the photograph of the organic sample with a superimposed contour plot of the photoresponse map at 632 nm. Good correlation of the discoloration features with the photocurrent map is evident.

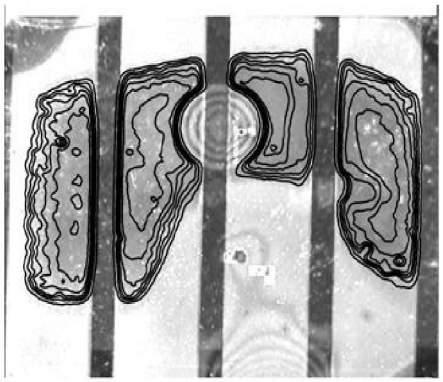

Figure 8. A contour plot of photoresponse map of an organic PV cell at 632 nm superimposed on a photograph of the cell.

Assembly Details

Two views of the set-up are shown in Figure 9 (and also in Figure 3).

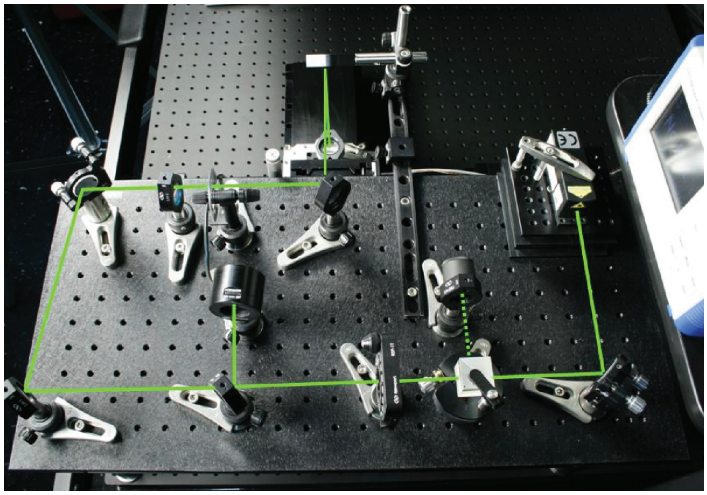

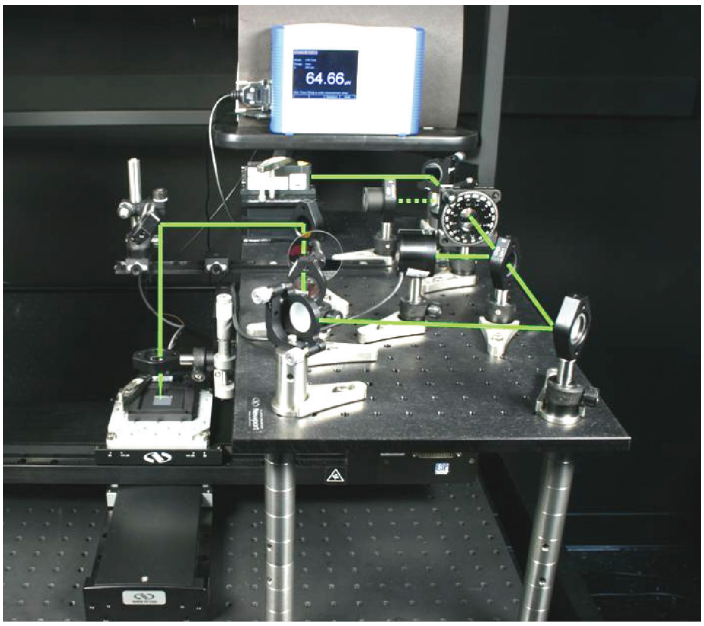

Figure 9. Photographs of the experimental device.

Assemble two stages (ILS250CC) in an XY configuration by removing the top plate of the lower stage and mounting the other stage on top of it using four M6 x 16 screws (screwing torque: 7 N.m / 62 in-Lbs). See Figure 10. See Section 9.0 of the ILS Series Manual for the XY assembly of the stages.

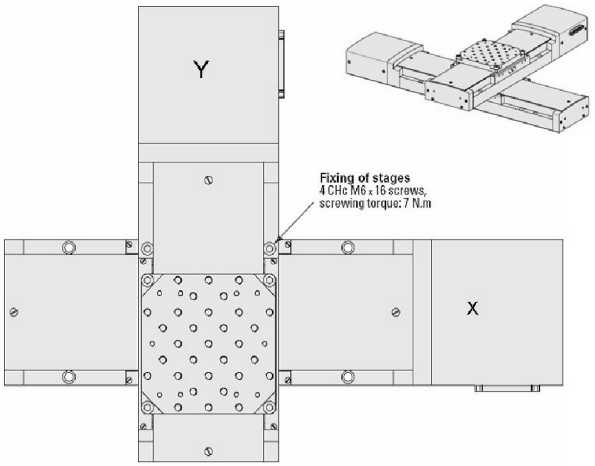

Figure 10. XY Motion stack using two ILS Series stages.

The motion stack should be securely attached to the working surface or bolted to the optical table. The photoresponse mapping kit is built on a plate 9" above the PV cell as shown in Figure 9. The cell is translated in the XY plane normal to the laser beam which is directed downward and focused onto the PV cell sample.

Connect the terminals of the sample cell to the input of the Oriel Preamplifier and its output to the first set of analog input pins of the GPIO2 port on the back of the XPS unit. See Figure 11. The XPS User's Manual has pin-I/O information. If a reference channel is used, then connect the analog output of the 1918-C power meter to the second set of analog input pins using the FK-18283 Adapter Cable (to be inserted into the analog output of the 1918-C). The individual stages of the XY stack will have to be set-up and configured. This is done by adding the stage names and parameters to the XPS configuration files stages.ini and system.ini before being used. Instructions on how to do this can be found in the XPS User's Manual.

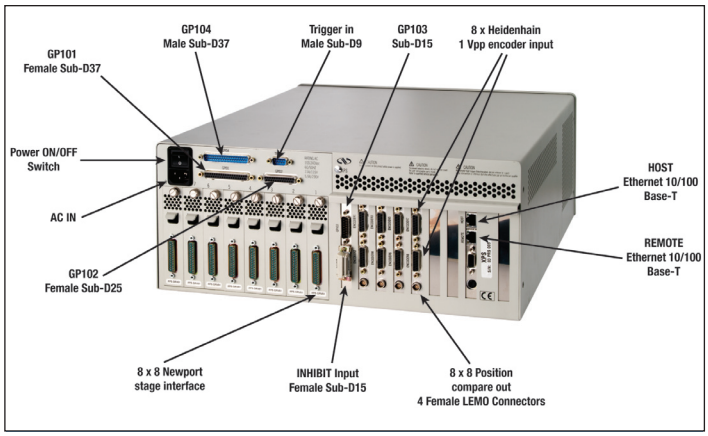

Figure 11. Rear panel of XPS Controller/Driver.

Using 8-32 set-screws connect the pedestal post (PS-4) and extensions (PS-4E, PS-1E) for four legs that will support the plate. Attach the legs to the SA-12 plate using TA-8Q20-10 thread adapters. Bolt the longer side of the 360-90 right angle bracket to the bottom center of the SA-12 to be flush with the edge of the SA-12. Assemble the 423 manual stage and the SM-25 micrometer and bolt this to the right angle bracket such that the micrometer is accessible from the top-side of the SA-12. This is used to adjust the lens L in Figure 2 and Figure 3 for the smallest spot size.

Place the SA-12 with attached legs onto the working surface so that it straddles the right half of the top (X-axis) stage as shown in Figure 9. Start building the plate up by mounting the laser to the plate. The height of the beam needs to be between 70 and 80 mm above the plate. Next, mount the routing mirrors at the three corners of the SA-12 plate leaving unused at least one or preferably two rows of threaded holes around the edges of the plate. Additional optics are used to route the beam downward through the SPX016 plano-convex lens and onto the sample PV cell.

Once the beam is routed down and focused onto the PV cell, the isolator optics can be inserted into the beam path. Mount the UGP-1 (for holding the polarizing beamsplitter) to the SA-12 plate and center the beamsplitter in the beam path. The rejected beam is captured with a PL15 beam dump. After the polarizing beamsplitter, place the 1/4 wave plate (10RP54-1) into the beam. The use of an isolator is especially important with a diode laser source to avoid modulation of the diode with optical feedback from the specular surface of the sample cell. A beamsplitter can be placed behind the 1/4 wave plate in order to provide a reference channel. For extra accuracy, the example software provided allows use of the reference channel for the purposes of dividing out any fluctuations in the laser source.

Software

The user interface of the software is shown in Figure 12.

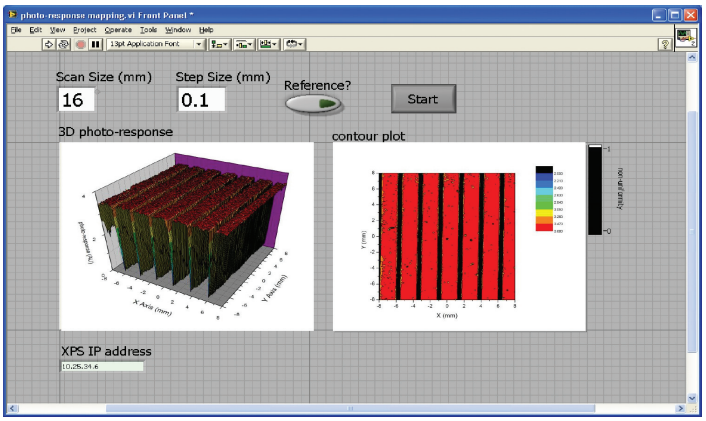

Figure 12. The example software user interface is shown. A 16mm x 16mm scan is shown.

Enter the scan and step size, and the software will display a 3D surface and contour plot of the photoresponse as data is collected. The scan data is saved as a matrix to a spreadsheet file. If the "Reference?" button is activated, three matrices will be recorded to file: one matrix contains normalized data, another contains raw data, and a third contains reference detector data. The software communicates with the XPS Motion Controller/Driver through a TCP/IP connection. The IP address of the XPS controller is entered in the user interface.

References

1. "Standard Test Methods for Electrical Performance Cells Using Reference Cells Under Simulated Sunlight," ASTM International, Vol. **E** 948-05a, (2005).

2 Sites, James et al., "Physical Characterization of Thin-film Solar Cells," Prog. Photovolt: Res. Appl. **12**, 177-217 (2004).

3 Martin,J., Fernandez-Lorenzo, C.,Poce-Fatou, J. A., and Alcantara,R., "A Versatile Computer-controlled High-resolution LBIC System," Prog. Photovolt: Res. Appl. **12**, 283-295 (2004).

4 Sawyer, W. D., "An improved method of light-beam-induced current characterization of grain boundaries," J. Appl. Phys. **59 (7)**, 2361-2363 (1986).

5 Hiltner, J. F. and Sites, J. R., "High resolution laser stepping measurements on polycrystalline solar cells," in 16th European Photovoltaic Solar Energy Conference (Glasgow, May 2000).

6 Jeranko, T., Tributsch,H., Sariciftci, N. S., Hummelen, J. C., "Patterns of efficiency and degradation of composite polymer solar cells", Solar Energy Materials & Solar Cells **83**, 247-262 (2004)

Newport Corporation

Worldwide Headquarters
1791 Deere Avenue
Irvine, CA 92606

(In U.S.): 800-222-6440
Tel: 949-863-3144
Fax: 949-253-1680

Email: sales@newport.com

Newport
Experience | Solutions

Visit Newport Online at: **www.newport.com**

This Application Note has been prepared based on development activities and experiments conducted in Newport's Technology and Applications Center and the results associated therewith. Actual results may vary based on laboratory environment and setup conditions, the type and condition of actual components and instruments used and user skills.

Nothing contained in this Application Note shall constitute any representation or warranty by Newport, express or implied, regarding the information contained herein or the products or software described herein. Any and all representations, warranties and obligations of Newport with respect to its products and software shall be as set forth in Newport's terms and conditions of sale in effect at the time of sale or license of such products or software. Newport shall not be liable for any costs, damages and expenses whatsoever (including, without limitation, incidental, special and consequential damages) resulting from any use of or reliance on the information contained herein, whether based on warranty, contract, tort or any other legal theory, and whether or not Newport has been advised of the possibility of such damages.

Newport does not guarantee the availability of any products or software and reserves the right to discontinue or modify its products and software at any time. Users of the products or software described herein should refer to the User's Manual and other documentation accompanying such products or software at the time of sale or license for more detailed information regarding the handling, operation and use of such products or software, including but not limited to important safety precautions.

This Application Note shall not be copied, reproduced, distributed or published, in whole or in part, without the prior written consent of Newport Corporation.

Newport Corporation, Irvine, California, has been certified compliant with ISO 9001 by the British Standards Institution.

MM#9000100
DS-010916